CHAPTER V

Porous Zinc Electrode Prepared from Zinc-Graphite-Natural Biodegradable Polymer Paste: Characterization and Application in the Zinc-Air Cell.

5.1 Introduction

The remaining aspects of the improvement of the zinc/gelled-electrolyte/air cell that are to be considered in the present work are the use of a porous zinc electrode and employing a substantially higher concentration of the KOH electrolyte. By providing an enhanced and intimate interfacial area per unit volume, the porous electrode increases the kinetics and mass transfer of the electrochemical reaction. This would lead to the decrease in the current density, better electrode rate capability, improved active material utilization, thus minimizing the energy loss [*Bagshaw, 1997; Newman and Tiedemann, 1975*]. Therefore, the development of porous electrodes has been the centre of interest in the development of batteries and fuel cells [*Jin and Lu,2001; Kriegsmann and Cheh, 1999; Lasia, 1995; Lasia, 1997; Lindbergh, 1997; Marozzi and Chialvo, 2000; Novak et. al, 1997; Periasamy et. al, 1996*].

Porous zinc electrodes are prepared in a number of different ways. For example, electrodeposited from an aqueous electrolytic bath [*Barbic et. al, 1999; Himy,*

1986]; roll-bonded process where a mixture of zinc, graphite, binder and solvent is extruded into a thin sheet [*Coates et. al, 1997*]; compressed dry powder process where a powder mixture of zinc and binder is placed in a mold and compressed around a current collector [*Himy, 1986; Zhu and Zhou, 1998*]; and paste or slurry preparation technique where powdered zinc oxide with gelling agent is mixed with KOH solution to form a paste and later applied onto a metal grid, dried and formed against a positive electrode in KOH solution [*Falk and Salkind, 1969; McBreen and Gagnon, 1981; Shivkumar et. al, 1998*].

In this work, porous zinc electrodes have been prepared from a mixture of zinc-graphite-gelatinized agar paste. When dried, the agar acts as a binder to the electrode. Graphite was included in the electrode composition in view of its favourable effects on the zinc electrode reported by several workers [*Bass et. al, 1988; Brown, 1983; Duffield et. al, 1987*]. The inclusion of conductive particulate graphite was reported to improve the zinc anode discharge capability, considerably inhibit active zinc dissolution and promote reprecipitation of oxidized zinc species [*Bass et. al, 1988; Brown, 1983; Duffield et. al, 1987*]. The graphite content and the agar solution concentration were varied to find the best electrode composition. The electrode performance was evaluated from the discharge capability of the zinc-air cells. The preparation of the porous zinc electrode adapted in this work is simple and fast, uses environmentally benign and biodegradable binding material, does not require either elevated heat treatment or mould and hydraulic press.

Previously, it has been shown that the application of a thin agar layer as an electrolyte reservoir between the electrode-gelled electrolyte interfaces enhanced the discharge capability of the cells outstandingly [*Othman et. al, 2001; Othman et. al, 2002*]. Though the porous electrode possesses a high surface area and sufficient amounts of KOH electrolyte normally entrapped within the electrode pores, the application of the thin agar layer between the electrode-gelled electrolyte interfaces is still beneficial to the cell discharge performance, as will be demonstrated in this work. Finally, a higher KOH concentration of 6 M was also employed, as the concentration of 2.8 M used throughout this work was comparatively low.

5.2 Experimental

5.2.1 Fabrication of the porous zinc electrode

A mixture of zinc and graphite powder was employed. The amount of graphite included was varied from initially 20-wt. % and finally reduced to 0-wt. %, whereas the amount of zinc powder used was fixed at 4.5 g. The zinc-graphite powder mixture was blended with 4 ml of gelatinized agar solution to form a paste. The agar solution concentration used was 5 mg cm^{-3}. The preparation of the gelatinized agar solution is as described previously in Section 4.32. The electrode paste was then cast onto a nickel-plated mesh that had been snugly fitted to a plastic holder and finally dried at a temperature of 50°C. The dried gelatinized agar solution acts as a binder to the zinc-graphite powder mixture. Agar solution concentrations of 15 mg cm^{-3}

and 25 mg cm^{-3} were also employed on the optimized zinc-carbon electrode composition.

5.2.2 Zinc-air cell assembly

Apart from the use of the fabricated porous zinc electrode, details of the cell components and assembly were similar to those described in Section 3.2. As normally zinc anode batteries comprise a KOH concentration in the range 6-10 M (27 to 40 wt.%) [*Bagotzky and Skundin, 1980*], a 6 M KOH concentration was also employed. In order to observe whether the use of the agar layer still improves the cell discharge performance, a similar approach to that described in Section 4.3.1 was employed, viz., (a) both the anode and cathode were agar coated, (b) only the zinc electrode was agar coated and finally (c) no agar coating was applied on either electrode.

5.2.3 Characterization of the porous zinc electrode

SEM micrographs, X-ray Diffraction measurement and particle size analysis were also performed on the porous zinc anode. The SEM micrographs were recorded using the Oxford 5431 SEM instrument. XRD measurements were undertaken using the Philips X-Ray Diffractometer XD-5 utilizing the Cu-K_α radiation (1.5405 Å). The particle size distribution of the zinc and graphite powders

used for porous electrode fabrication was analyzed using the Coulter LS 230 Particle Size Analyzer.

5.2.4 Characterization of the zinc-air cell

The fabricated zinc-air cell was characterized according to its operating voltage vs. current drain and power density curves, and discharge profile at constant current of 50 and 100 mA. A LG-50 Galvanostat electroanalytical system was used to perform the experiments.

5.3 Results

The mean particle sizes of the zinc and graphite powders utilized in the fabrication of the porous electrode were 12 μm and 18 μm respectively. The cross sectional view of the porous electrode that consists of the powder mixture of zinc and graphite is given in Figure 5.1. It reveals the occurrence of two distinct layers. Closer observation of the darker region reveals that it is a graphite-rich matrix (refer to Figures 5.2a and 5.2b). Figures 5.3a to 5.3b show the cross-sectional view of the porous zinc electrode that consists of zinc powder only at different magnifications. Note the whitish trace of the dried agar that acts as a binder to the zinc powder.

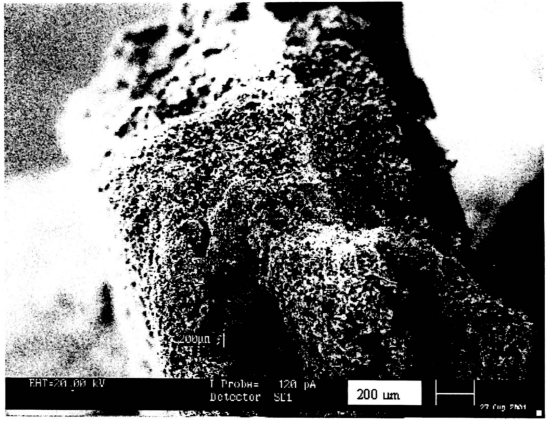

Figure 5.1. SEM cross-sectional view of the porous zinc electrode prepared from the zinc-graphite-agar paste indicating the occurrence of two distinct layers.

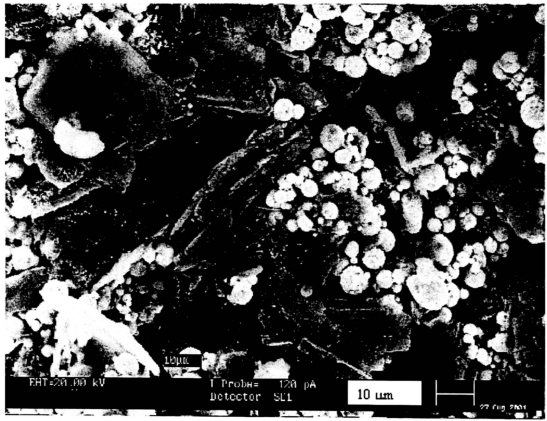

Figure 5.2 (a). A closer observation on the darker region reveals that it is a graphite-rich layer.

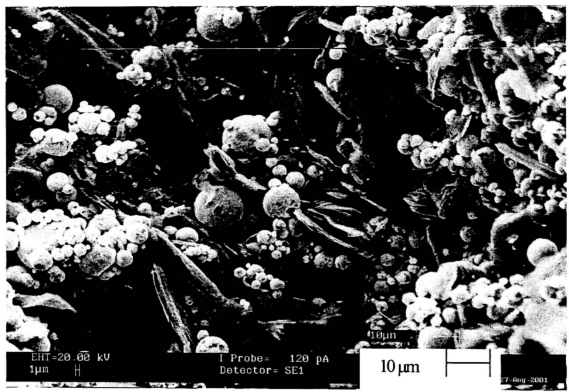

Figure 5.2 (b). Another SEM micrograph of the graphite-rich layer taken from other spot.

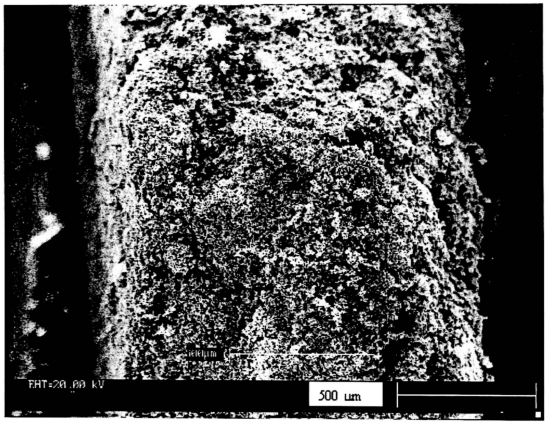

Figure 5.3 (a). SEM cross-sectional view of the optimized porous zinc electrode that consists of zinc powder only.

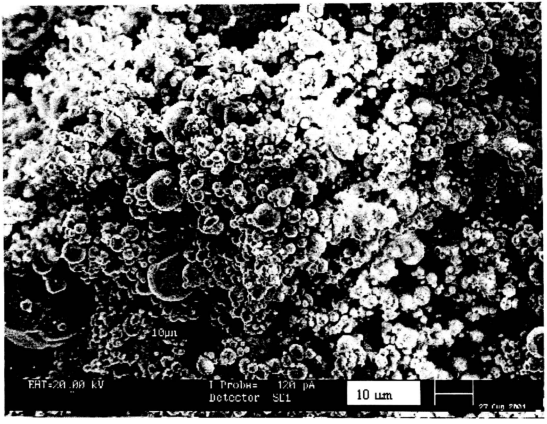

Figure 5.3 (b). A closer cross-sectional view of the porous zinc electrode. Most probably the whitish traces are due to the dried agar.

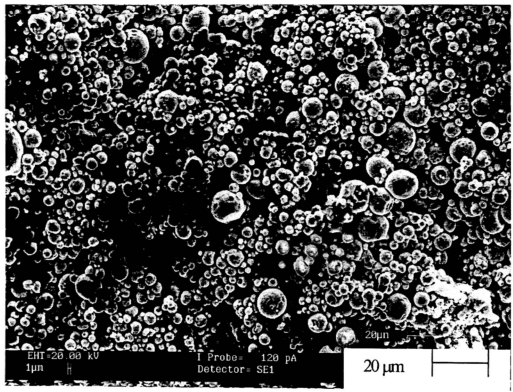

Figure 5.3 (c). SEM micrograph showing the porous nature of the fabricated zinc electrode.

The optimum composition of the porous zinc electrode was evaluated from the cell discharge capability. The variation in the cell discharge capacity as the graphite content in the zinc electrode was varied is shown in Figure 5.4. It is interesting to note that the cell capacity registers a maximum of 1349 mAh when there was no graphite content in the zinc electrode. Further, the cell capacity decreases with increasing graphite content until 10-wt. %, after which the cell capacity is constant.

The discharge performance of the cells with different agar solution concentration of 5, 15 and 25 mg cm^{-3}, is given in Figure 5.5. In the preparation of these electrodes, no graphite was incorporated. It clearly shows that the best discharge performance is obtained from the zinc anode employing the 5 mg cm^{-3} agar concentration. Below 5 mg cm^{-3} concentration, the resulting solution was too dilute or watery and hence it was not applied in the electrode fabrication. Figure 5.6a depicts the cross-sectional electron micrograph of the porous zinc electrode in which a higher agar solution concentration of 15 mg cm^{-3} was employed. Notice that the dried agar film formed, encapsulated some portion of the electrode active material. Figures 5.6b and 5.6c give clearer view at higher magnification taken from other spots.

For comparison, Figure 5.7 displays the outstanding discharge performance of the zinc-air cell with the porous zinc anode compared to that using the compact planar zinc foil rated at 50 mA.

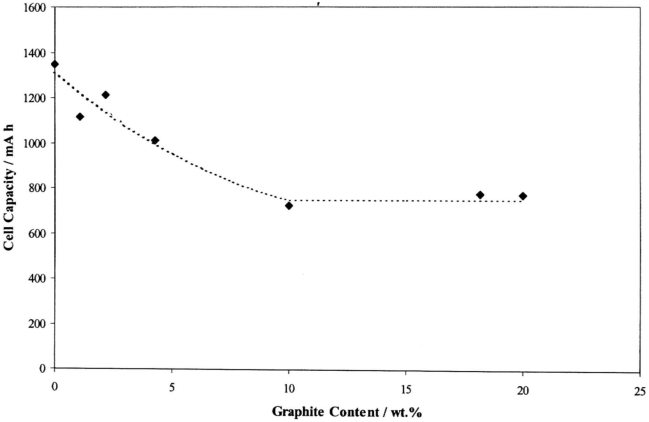

Figure 5.4. The influence of graphite content in the zinc electrode composition on the zinc-air cell capacity.

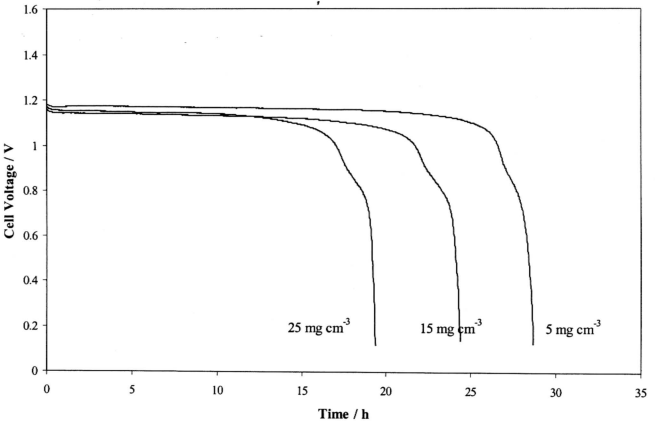

Figure 5.5. Zinc-air cell discharge profiles showing the influence of the agar solution concentration to the discharge performance.

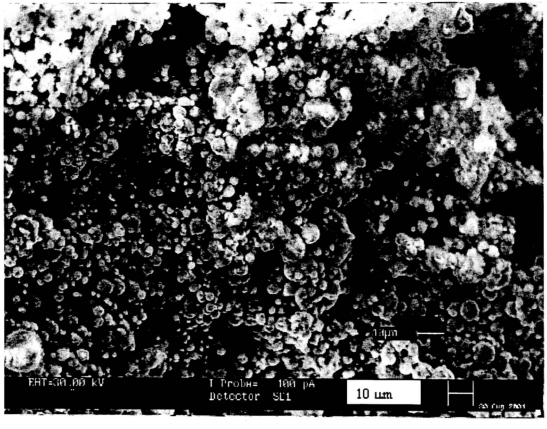

Figure 5.6 (a). Electron micrograph showing the formation of the agar film that shields some portion of the zinc active material.

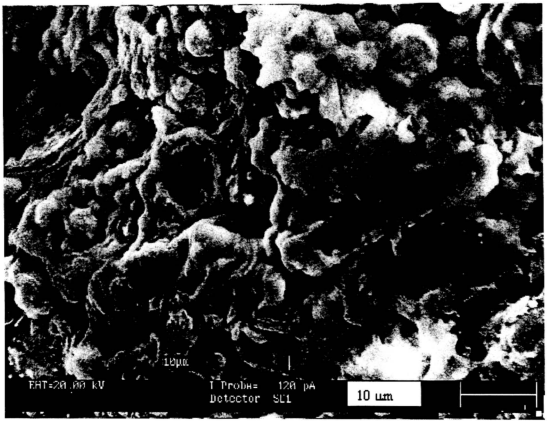

Figure 5.6 (b). An obvious view indicating the formation of the agar film that encapsulates the active material.

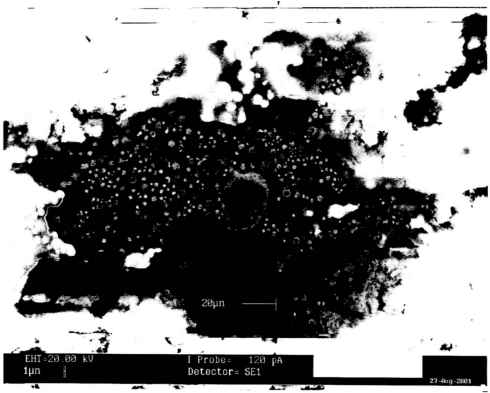

Figure 5.6 (c). Another example showing the formation of the agar layer.

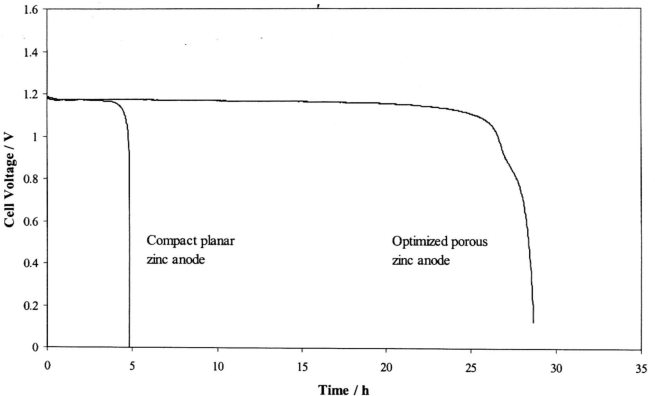

Figure 5.7. Discharge profiles of the zinc-air cell employing the optimized porous zinc electrode as compared to that using the compact planar zinc foil.

These results were obtained employing the KOH concentration of 2.8 M. Finally, a higher KOH concentration of 6 M was employed and as anticipated, enhanced discharge capability of the cell was obtained (see Figure 5.8). Better operating voltage-current drain profile was also observed, as shown in Figure 5.9.

The application of a thin agar layer between the electrode-gelled electrolyte interfaces essentially improves the cell discharge performance. As shown in Figure 5.10, the cell capacity improves by 28 % as an agar layer was introduced between the zinc anode-gelled electrolyte interface, and it is further enhanced by 52 % when the agar layer was applied onto both electrode-gelled electrolyte interfaces. These profiles were obtained at 100 mA discharge current and employing a 6 M KOH electrolyte.

Electron micrographs of the discharged porous zinc electrode show that the zinc particles are covered with crystals that are possibly of zinc oxide (Figure 5.11a and 5.11b). The XRD analysis (refer Figure 5.12) of the post-discharge electrode matches that of zinc oxide [*Izaki and Omi, 1997; ASTM 5-0664, 1967*], which confirms the SEM observations. Zinc oxide is the end product of the zinc-air cell electrochemical reaction.

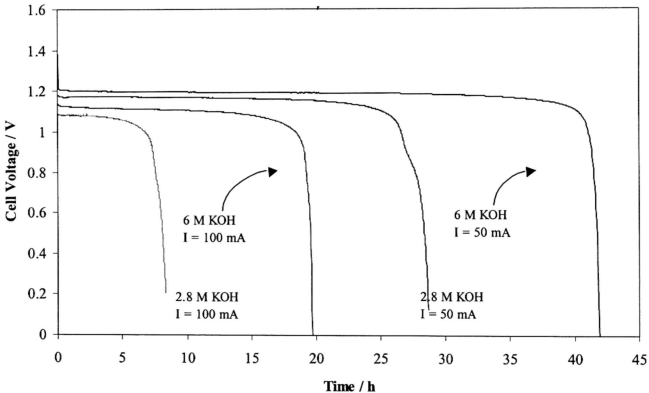

Figure 5.8. Comparison of the discharge performance of the zinc-air cell employing the 2.8 and 6 M KOH concentrations.

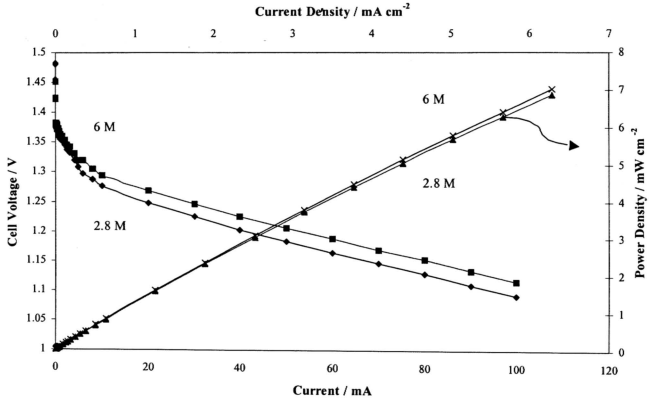

Figure 5.9. Operating voltage versus discharge current profiles of the zinc-air cell employing the 2.8 and 6 M electrolyte concentrations and the corresponding power density profiles.

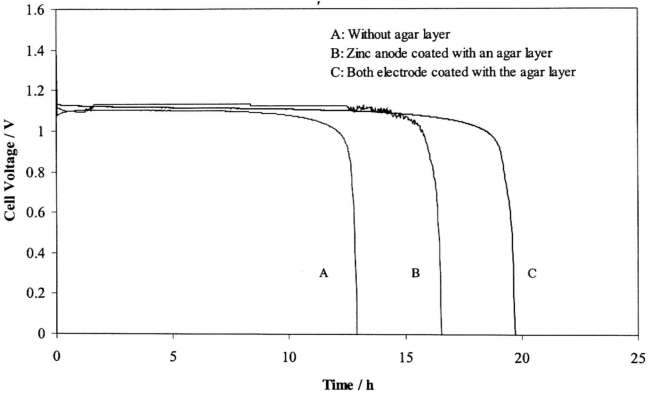

Figure 5.10. Zinc-air cell discharge profiles indicating the influence of agar-coating on the cell discharge performance.

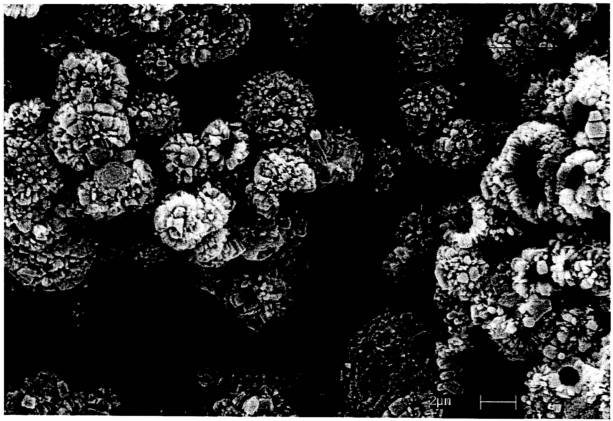

Figure 5.11 (a). Post-discharge SEM micrograph of the porous zinc electrode exhibit the zinc particles are covered with zinc oxide crystals

Figure 5.11 (b). SEM micrograph of the zinc oxide crystals at higher magnification (10000x).

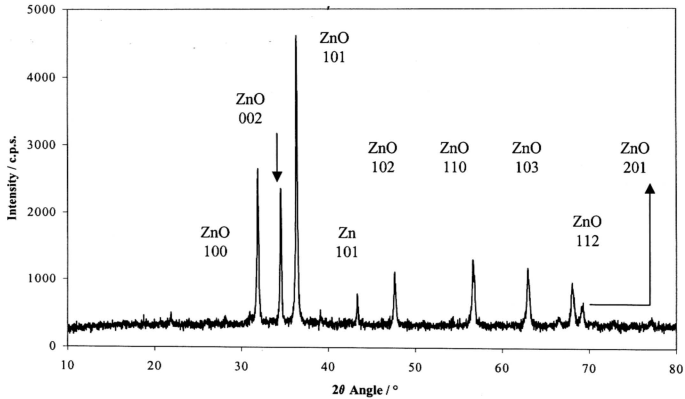

Figure 5.12. XRD pattern of the porous zinc electrode after complete discharge that matches to that of zinc oxide.

5.4 Discussion

Several workers have reported favourable results on the inclusion of particulate graphite into the zinc electrode [*Bass et. al, 1988; Brown, 1983; Duffield et. al, 1987*]. The conductive particulate graphite was reported to improve zinc anode discharge capability, considerably inhibit active zinc dissolution and promote reprecipitation of oxidized zinc species [*Bass et. al, 1988; Brown, 1983; Duffield et. al, 1987*]. However, in the present study, an optimum cell capacity of 1349 mAh was obtained for the electrode without graphite content and, in fact, the cell capacity decreases with increasing graphite content. This observation might be attributed to the existence of two distinct layers in the electrode structure and also the use of the gelled electrolyte. Graphite, with its density significantly lower than zinc, surfaces and forms a graphite-rich matrix in the electrode structure. As a result, the formation of the graphite-rich layer obscures the electrode wettability and porosity, and hence reduces the cell capacity. The use of gelled KOH in the form of semi-solid jelly granules further exacerbates this phenomenon due to the limited free electrolyte nature of the gelled electrolyte.

Another factor that might contribute to the formation of the graphite-rich layer is the agar solution concentration. A more viscous gelatinized agar solution most probably blends the zinc and graphite mixture homogeneously. Nevertheless, the electrode fabricated from the zinc powder that utilized higher agar solution concentrations of 15 mg cm^{-3} and 25 mg cm^{-3}, resulted in reduced cell capacities,

though it improved the electrode's mechanical stability and strength. At these solution concentrations, the dried agar forms a film that is thick enough to shield the zinc active material and thus reduce the active material utilization. The electron micrographs of the electrode utilizing 15 mg cm^{-3} agar solution concentration clearly revealed this phenomenon.

The porosity of the optimized zinc electrode was estimated at around 60 %. The thickness of the optimized porous zinc electrode was approximately 1.0 mm as estimated from the cross sectional electron micrograph. Thus the porosity of the electrode is calculated as follows,

$$\frac{V_{Pore}}{V_{Total}} \times 100\% = \frac{V_{Total} - V_{Zn}}{V_{Total}} \times 100\% = \left\{1 - \frac{m_{Zn}/\rho_{Zn}}{\pi r^2 h}\right\} \times 100\%$$

where,

V_{pore}; Total pores volume within the electrode

V_{Total}; Total electrode volume

V_{Zn}; Total volume occupied by the zinc active material

m_{Zn}; zinc active material total mass

ρ_{Zn}; zinc density (7.13 g cm^{-3})

r; electrode radius

h; electrode thickness

Though the fabricated zinc electrode was highly porous and thus contributed to a high specific surface area, the application of the agar layer was still essentially useful to the cell discharge performance. As mentioned earlier, the role of agar as an electrolyte reservoir, improves both the wettability and the electrode-gelled electrolyte interfacial contact.

Zinc-air cells with practical capacity of 1910 mAh (420 Wh kg^{-1}) and 2066 mAh (443 Wh kg^{-1}) rated at continuous current drain of 0.1 A and 50 mA, respectively, have been accomplished in this work. Based on the 4.5-g (4.5/65.37 mole) zinc active material and considering zinc oxide (81.37×10^{-3} kg mol^{-1}) as the end product of the electrochemical reaction, the cell specific energy density is calculated as follows:

$$\frac{\{practical\ cell\ capacity\,(Ah)\} \times \{average\ operating\ voltage\,(\tilde{V})\}}{\{amount\ of\ discharge\ product\,(kg)\}}$$

5.5 Summary

A porous zinc anode of 60 % porosity has been fabricated from zinc powder using gelatinized algal polysaccharide solution as a binder. The technique employed was simple and fast and requires neither elevated heat treatment nor mould and hydraulic press. At 5 mg cm^{-3} agar solution concentration, the inclusion of particulate graphite into the electrode does not improve its performance. The

particulate graphite surfaces and forms a graphite-rich layer that obscures the electrode porosity. The application of a thin agar layer between the electrode-gelled electrolyte interfaces in the cell design improves the cell discharge performance significantly. The zinc-air cell employing the optimized porous electrode has demonstrated a practical capacity of 2066 mA h and specific energy density of 443 Wh kg^{-1}.

References

ASTM X-Ray Powder Data File, J.V. Smith (Editor), Inorganic Vol., American Society for Testing and Materials (ASTM) **(1967)** 5-0664

Bagotzky, V.S. and Skundin, A.M., Chemical Power Sources, Academic Press **(1980)** Chap. 12

Bagshaw, N.E., "Improving active-material utilization", J. Power Sources 67 **(1997)** 105-109

Barbic, P.A., Binder, L., Voss, S., Hofer, F. and Grogger, W., "Thin film zinc/manganese dioxide electrodes based on micropolymer", J. Power Sources 79 **(1999)** 271-276

Bass, K., Mitchell, P.J., Wilcox, G.D. and Smith, J., "The electrodeposition of zinc onto graphitic carbon substrates from alkaline electrolytes", J. Power Sources 24 **(1988)** 21-29

Brown, D.J., "Secondary zinc electrode", United States Patent 4,407,915 **(1983)**

Coates, D., Ferreira, E. and Charkey, A., "An improved nickel/zinc battery for ventricular assist systems", J. Power Sources 65 **(1997)** 109-115

Duffield, A., Mitchell, P.J., Shield, D.W. and Kumar, N., in: in: Power Sources 11, Proceedings of the 15th International Symposium on 'Research and Development in Non-Mechanical Electrical Power Sources 1986', Pearce, L.J. (Editor), Academic Press Inc. International Power Sources Symposium Committee, Leatherhead, UK **(1987)** pg. 253-279

Falk, S.U. and Salkind, A.J., Alkaline Storage Batteries, John Wiley and Sons Inc. (**1969**) Chap. 3

Himy, A., Silver-Zinc Battery: Phenomena and Design Principles, 1st Ed., Vantage Press (**1986**) Chap. 4

Izaki, M. and Omi, T., "Characterization of transparent zinc oxide films prepared by electrochemical reaction", J. Electrochem. Soc., 144 (**1997**) 1949-1952

Jin, X. and Lu, J., "Simplified methods for determining the ionic resistance in a porous electrode using linear voltammetry," J. Power Sources 93 (**2001**) 8-13

Kriegsmann, J.J. and Cheh, H.Y., "The effect of cathode porosity on the performance of a cylindrical alkaline cell", J. Power Sources 77 (**1999**) 127-135

Lasia, A., "Impedance of porous electrodes", J. Electroanal. Chem. 397 (**1995**) 27-33

Lasia, A., "Porous electrodes in the presence of a concentration gradient", J. Electroanal. Chem. 428 (**1997**) 155-164

Lindbergh,G., "Experimental determination of the effective electrolyte conductivity in porous lead electrodes in the lead-acid battery", Electrochim. Acta 42 (**1997**) 1239-1246

Marozzi,C.A. and Chialvo, A.C., "Development of electrode morphologies of interest in electrocatalysis. Part 1: Electrodeposited porous nickel electrodes", Electrochim. Acta 45 (**2000**) 2111-2120

McBreen, J. and Gagnon, E., "The electrochemistry of metal oxide additives in pasted zinc electrodes", Electrochim. Acta 26 (**1981**) 1439-1446

Newman, J. and Tiedemann, W., "Porous-electrode theory with battery applications", AIChE J. 21 (**1975**) 25-41

Novak, P., Scheifele, W., Winter, M. and Haas, O., "Graphite electrodes with tailored porosity for rechargeable ion-transfer batteries", J. Power Sources 68 (**1997**) 267-270

Othman, R., Yahaya, A.H. and Arof, A.K., "Zinc-air cell with KOH-treated agar layer between electrode and electrolyte containing hydroponics gel", in: New Materials for Electrochemical Systems IV, Savadogo, O. (Editor), Extended Abstract of the 4th International Symposium on New Materials for Electrochemical Systems, 9-13 July, 2001, Montreal, Quebec, Canada, Ecole Polytechnique de Montreal (**2001**) pg. 300-303

Othman, R., Yahaya, A.H. and Arof, A.K., "Zinc-air cell with KOH-treated agar layer between electrode and electrolyte containing hydroponics gel", J. New Mat. Electrochem. Systems 5 (**2002**) 177-182

Periasamy, P., Babu, B.R. and Iyer, S.V., "Cyclic voltammetric studies of porous iron electrodes in alkaline solutions used for alkaline batteries", J. Power Sources 58 (**1996**) 35-40

Shivkumar, R., Kalaignan, G.P. and Vasudevan, T., "Studies with porous zinc electrodes with additives for secondary alkaline batteries", J. Power Sources 75 (**1998**) 90-100

Zhu, J-L. and Zhou, Y-H., "Effects of ionomer films on secondary alkaline zinc electrodes", J. Power Sources 73 (**1998**) 266-270